JOURNAL OF SOLID STATE CHEMISTRY **136,** 322–327 (1998)
ARTICLE NO. SC987810

LETTER TO THE EDITOR

Large Magnetoresistance Effects in Self-Doped $La_{0.936}Mn_{0.982}O_3$ Single Crystals

W. H. McCarroll

Department of Chemistry, Rider University, Lawrenceville, New Jersey 08648

K. V. Ramanujachary[1] and M. Greenblatt

Department of Chemistry, Rutgers University, Piscataway, New Jersey 08854-8087

and

F. Cosandey

Department of Ceramic and Materials Engineering, Rutgers University, Piscataway, New Jersey 08854-8087

Communicated by J. M. Honig February 10, 1998; accepted February 17, 1998

We report here for the first time colossal magnetoresistance effects (~77% MR at 5 T) in bulk single crystals of self-doped $La_{0.936}Mn_{0.982}O_3$ prepared by fused-salt electrolysis. The crystals form with rhombohedral symmetry and show a high degree of perfection by electron backscatter diffraction. The maximum in the MR% was observed in the vicinity of ~250 K where the crystals undergo a sharp insulator-to-metal as well as a paramagnetic-to-ferromagnetic transition. © 1998 Academic Press

INTRODUCTION

The discovery of colossal magnetoresistance (CMR) effect in several perovskite oxides in the *Ln*–*A*–Mn–O system (*Ln* = rare earth ion, *A* = di- or monovalent cation) has spurred intense research effort because of its relevance to magnetic data storage and retrieval technologies (1–6). Until recently, it was suggested that the double-exchange mechanism of Zener, which requires a mixed valent Mn^{3+}/Mn^{4+} couple, is responsible for the CMR effect in $Ln_{1-x}A_xMnO_3$ compounds (7). However, recent discoveries of the CMR effect in $Tl_2Mn_2O_7$ (with Mn exclusively in the 4+ state) (8) and the thio-spinels $Fe_{1-x}Cu_xCr_2S_4$ ($x = 0$ and 0.5) (9) seem to indicate that the mechanism responsible for the CMR effect is more complicated than originally proposed.

Another important aspect of the CMR of manganates is that most experimental investigations reported in the literature are on ceramic specimens or thin films grown on both poly- and single-crystal substrates. Efforts to examine the MR effects in bulk single-crystal specimens have been scarce, because the crystal growth of perovskite manganates is cumbersome, requiring the use of specialized apparatus for generating very high temperatures which are not accessible in most laboratories (10, 11). There have been reports in the literature indicating that the MR effect is dominated by grain boundary (GB) effects at least at $T \ll T_c$, and that the MR is much larger in polycrystalline samples than in single-crystal specimens due to carrier scattering and the modification of the magnetic structure near the grain boundaries (12–15).

Recently we reported on the synthesis and properties of crystals of doped lanthanum manganates with a rhombohedral perovskite structure, which were prepared by electrochemical means at a relatively low temperature (<1000°C) and in air from melts of Na_2MoO_4–MoO_3 solvent mixtures (16). These crystals also contained up to 7 mol% Al, which had been abstracted from the alumina crucible used to contain the melt. Since then, we have succeeded in growing good quality single crystals of undoped lanthanum manganate suitable for magnetic and transport measurements using molten $Cs_2MoO_4 + MoO_3$ mixtures as solvents. Here we report our results on the synthesis, characterization, and magnetoresistive properties of these crystals.

[1] Present address: Chemistry Department, Rowan University, Glassboro, NJ 08028.

0022-4596/98 $25.00

EXPERIMENTAL

Only a brief description of the growth conditions will be given here, as the details can be found elsewhere (17). Briefly, the crystals were grown using the melts obtained from mixtures of pre-dried Cs_2MoO_4 and MoO_3 to which $MnCO_3$ and La_2O_3 were added. Electrolysis was carried out in air using Pt electrodes at temperatures in the range 975–1000°C. Yttria stabilized zirconia crucibles were used to contain the melt. When the electrolyses were carried out using a current of 10–15 mA for four-to-five days, crystals of cubic-like habit up to 3–5 mm on edge were obtained. The crystals were mechanically separated from the anode and subsequently washed with a warm solution of dilute K_2CO_3 containing a small amount of disodium ethylenediaminetetraacetic acid.

Chemical analysis for La and Mn contents were made with a Baird Atomic Model 2070 inductively coupled plasma emission spectrometer (ICP). Cs analysis was carried out by atomic absorption spectrometry. The average valence of Mn was determined by an iodometric technique which employs an amperometric dead-stop end point technique (18). Powder X-ray diffraction (PXD) data were collected with a Rigaku D-Max 2 system and graphite monochromatized Cu$K\alpha$ radiation.

Crystal orientation with submicrometer spatial resolution was determined in a scanning electron microscope (SEM) by recording the electron backscatter diffraction pattern (EBSD) with an Oxford Opal CCD camera. Details of the EBSD technique can be found elsewhere (19).

The electrical resistivity measurements were made with a closed-cycle refrigeration system in a four-probe configuration down to 30 K. Magnetization and magnetoresistance were measured with a Quantum Design Squid Magnetometer (MPMSR2). All the above physical characterizations were carried out on the same single crystal.

RESULTS AND DISCUSSION

Figure 1 shows an example of some of the larger crystals and agglomerates, which were mechanically separated from a larger agglomerate grown on the Pt wire anode as shown in Fig. 2.

The powder X-ray diffraction pattern of the crushed single crystals could be indexed based on a rhombohedral unit cell (space group $R\bar{3}c$) with the cell parameters $a = 5.4816(3)$ Å, $\alpha = 60.656(6)^\circ$, $V = 118.19(1)$ Å^3. The equivalent parameters for a hexagonal triple cell are $a_h = 5.5359(3)$, $c_h = 13.360(8)$ Å and $V_h = 354.58(4)$ Å^3. ICP analysis for possible contaminants such as Na, Al, Mo, Pt, Si, Y, and Zr, showed, with the exception of Na and Y, that they were present at levels of $<0.02\%$ by weight while Na and Y were somewhat higher at 0.05%. Cs was at ppm levels. The chemical formula for the crystals based upon triplicate analyses for La, Mn and average manganese valence was found to be $La_{0.936}Mn_{0.982}O_3$. The Y content represents less than 0.1 atomic percent of the large cation site occupancy and has not been included in the formula. The Na content of 0.05% is noticeably high, but may have been inadvertently introduced in the sample dissolution or analysis procedure, given the ubiquitous nature of this element. The oxygen content was estimated using the experimentally determined Mn valency, since the perovskite structure tolerates cation deficiency rather than anion excess (20–22). The lanthanum and manganese deficiency in these crystals, as expected, induces mixed-valency at the Mn site, resulting in the Mn^{3+}/Mn^{4+} couple.

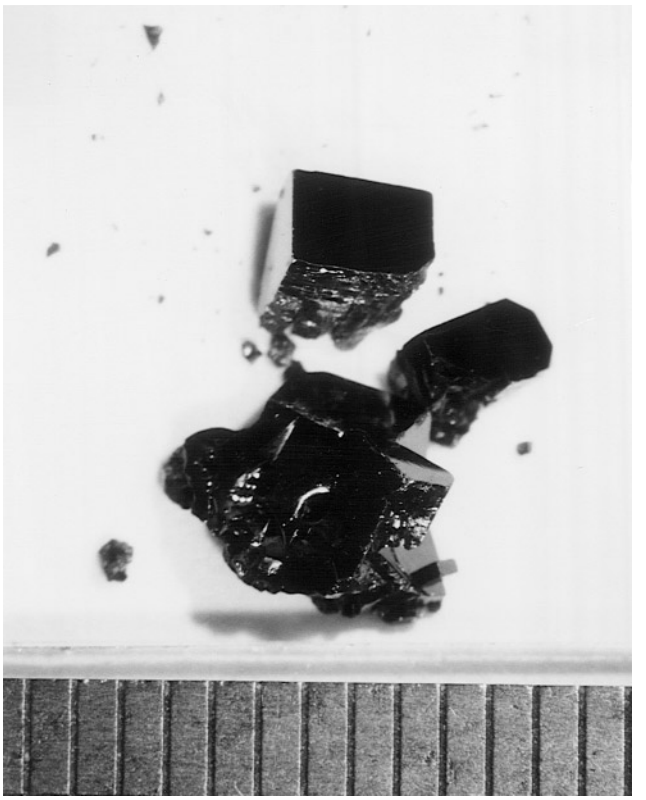

FIG. 1. Crystal fragments of $La_{0.936}Mn_{0.982}O_3$ (mm scale shown for dimensions).

The perfection of individual crystals has been measured using EBSD by recording diffraction patterns along crystal surfaces at 100-micron intervals and by calculating the misorientation angle between patterns. A typical EBSD pattern is shown in Fig. 3a along with principal pole directions. The [0, −2, 2, 1] surface normal direction taken from many different areas is shown in Fig. 3b in a reduced stereographic triangle. Quantitative orientation determinations reveal misorientations of less than 1° between patterns indicative of highly perfect single crystals with only isolated dislocations forming low angle grain boundaries.

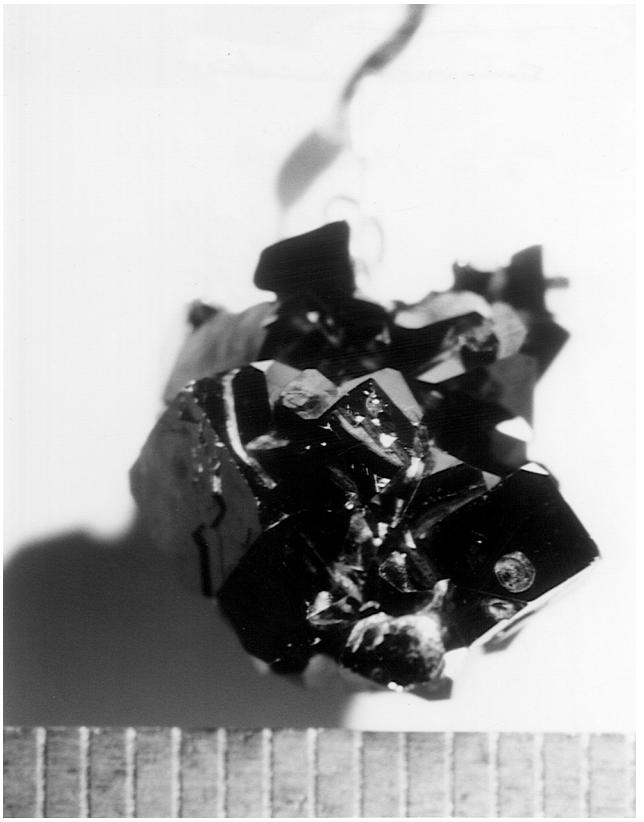

FIG. 2. An as-grown crystal agglomerate on the Pt wire anode.

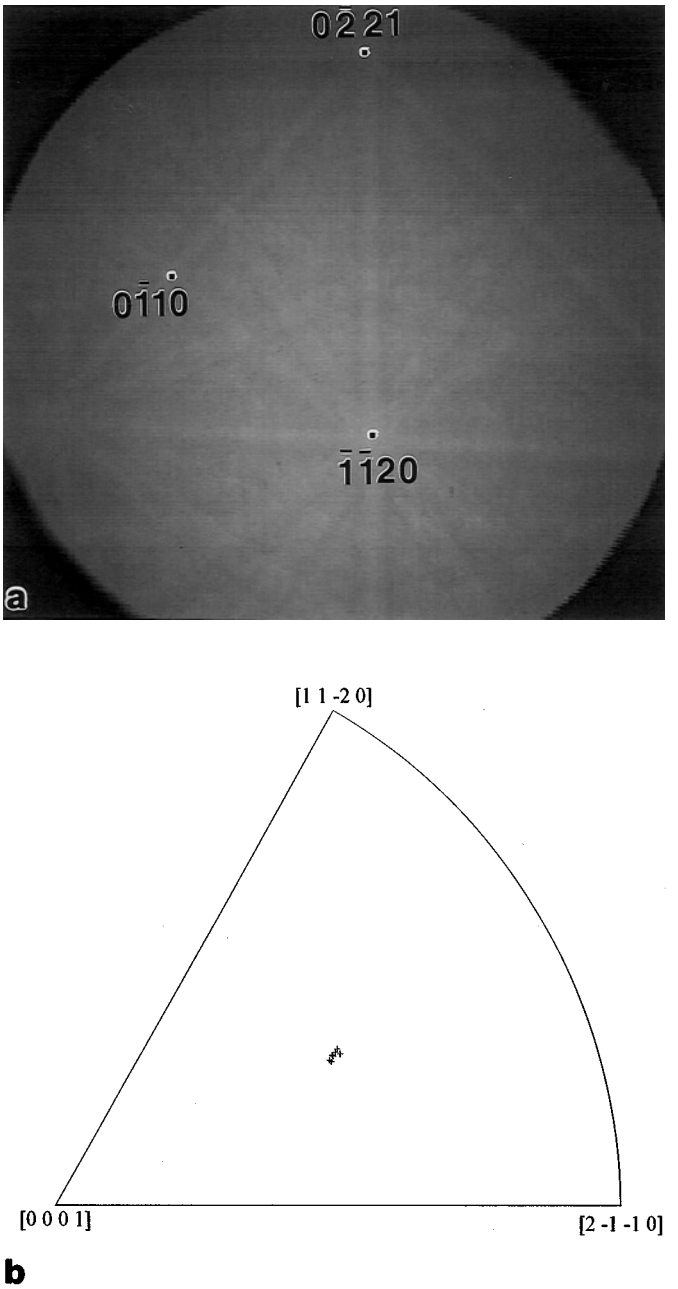

FIG. 3. (a) Typical EBSD pattern along with principal pole directions and (b) reduced stereographic triangle with [0, −2, 2, 1] surface normal directions taken along a 2-mm crystal face.

The magnetic susceptibility of a $La_{0.936}Mn_{0.982}O_3$ single crystal measured as function of temperature in Fig. 4 shows a sharp transition to the ferromagnetic state at ~ 250 K. The magnetization at $T < T_c$ remains invariant down to 2 K. This feature is significantly sharper than that observed in an epitaxially grown $La_{1-x}MnO_3$ film (23). In Fig. 5, we show the electrical resistivity (ρ) variation of the same crystal used in the magnetization measurements in the temperature range 30–300 K. The normal state resistivity of 2×10^{-1} Ω-cm near room temperature increases to $\sim 4 \times 10^{-1}$ Ω-cm when cooled down to ~ 240 K, and then decreases rapidly below this temperature. The insulator-metal transition temperature (T_{im}) being somewhat lower than the Curie temperature (T_c) from magnetization measurements is commonly observed in rare earth manganates (6). There appears to be an anomaly at ~ 200 K in Fig. 6, which was attributed to a rhombohedral-to-orthorhombic transition in $La_{1-x}Sr_xMnO_3$ (24).

The sharpness of the insulator-metal transition prompted us to investigate the magnetoresistive effect in these crystals and results of these studies are presented in Fig. 6. A maximum of 77% MR (%MR being defined as $[(r(0)-r(H))/r(0))] \times 100$, where $r(0)$ and $r(H)$ are the resistivities at an applied field of zero and H respectively), is observed in these crystals at ~ 250 K and 5 T (the maximum attainable field of our SQUID) applied field. Such high MR% are hitherto observed only in polycrystalline or single crystal compositions of doped rare earth manganates.

Of particular relevance in understanding the large magnetoresistance of the crystals is the formal valence of Mn and the geometry of the Mn–O–Mn network. In our crystals, the formal valence of manganese, as determined by

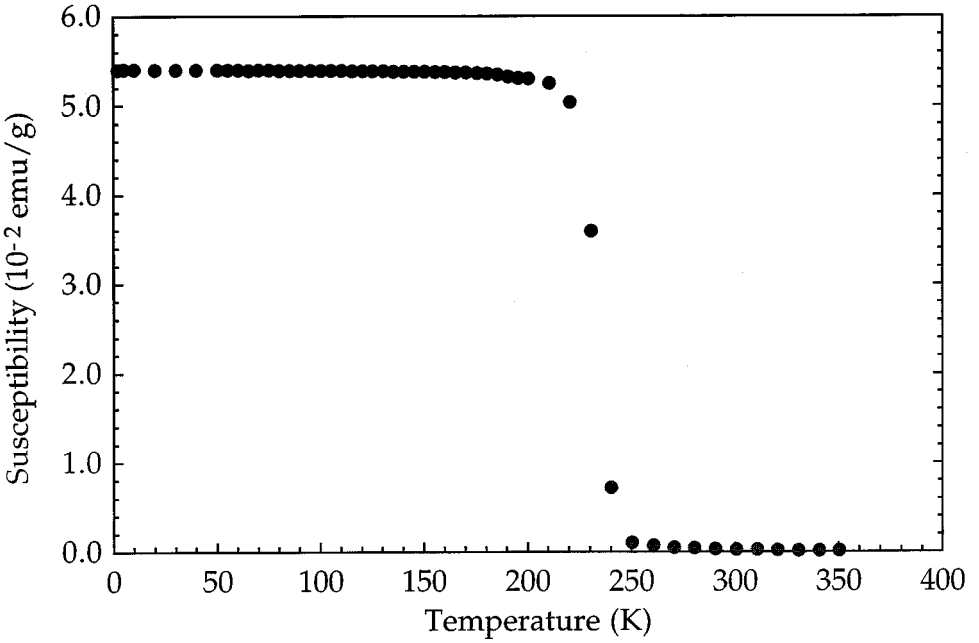

FIG. 4. Magnetic susceptibility of $La_{0.936}Mn_{0.982}O_3$ crystal as a function of temperature.

chemical analysis is 3.25, a value comparable to that reported for the $La_{0.75}Sr_{0.25}MnO_3$ single crystals (10). The latter is reported to have a T_c of $\sim$340 K, much higher than observed in our crystals ($\sim$250 K), although the unit cell symmetry is rhombohedral in both cases. This would indicate that the formal valence of Mn is not of itself the determining factor of T_c and/or T_{im} in rare earth manganates.

Ferris *et al.* (25) observed a second-order structural phase transition, $R\bar{3}c \leftrightarrow R3c$ at T_{im} in cation deficient $La_{1-x}MnO_3$ ($x = 0.0$, 0.05, 0.1). They report $T_{im} \sim T_c$ at

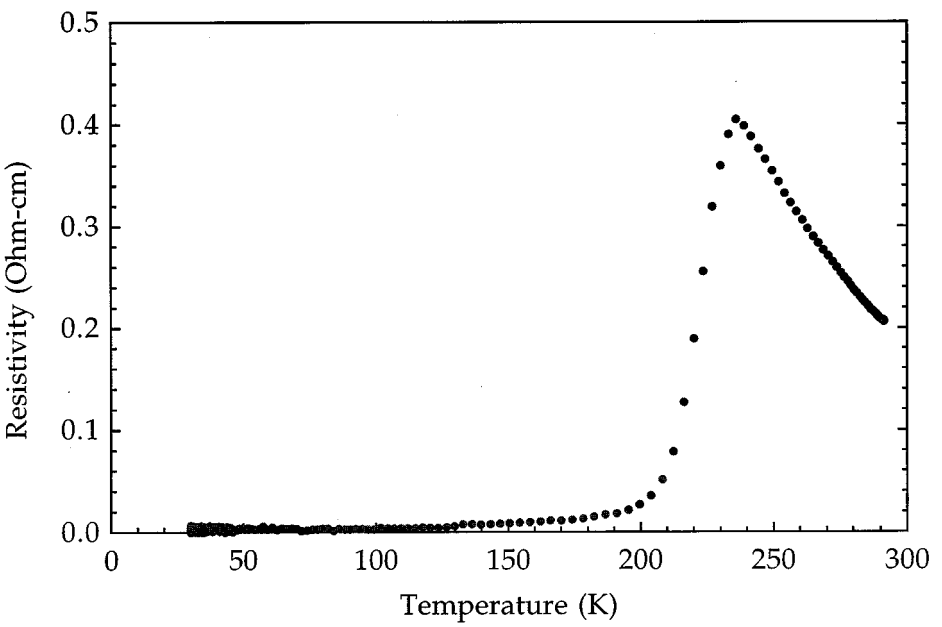

FIG. 5. Electrical resistivity variations of $La_{0.936}Mn_{0.982}O_3$ crystal as a function of temperature.

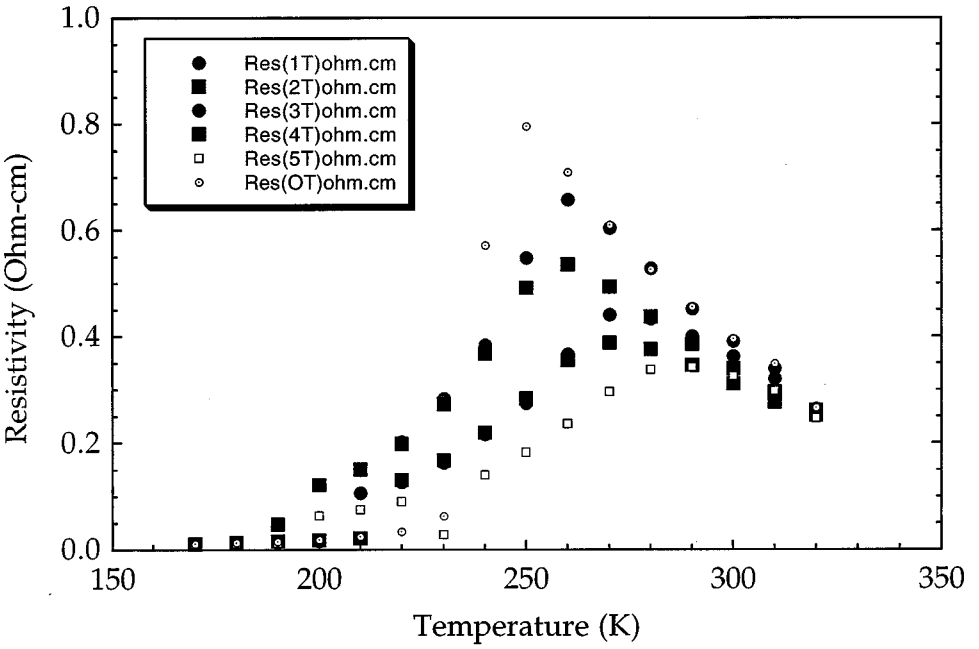

FIG. 6. Temperature- and field-dependent resistivities of the $La_{0.936}Mn_{0.982}O_3$ crystal.

250 K in their $La_{0.9}MnO_3$ composition, formulated as $La_{0.894}Mn_{0.993}O_3$, which is quite similar to the composition ($La_{0.936}Mn_{0.982}O_3$) of the single crystal manganate reported here.

Maignan *et al.* (26) have recently reported CMR properties in the polycrystalline $La_{0.9}MnO_{3-d}$ system which showed T_c's in the range 230–260 K. Although the PXD patterns of these samples are formally consistent with rhombohedral symmetry, the actual symmetry has been shown to be monoclinic by electron diffraction studies. The fact that our crystals showed MR ratios, T_c, and T_{im} values which also correspond closely to this monoclinic phase led us to carefully examine our PXD data. We examined a scan run from $2\theta = 18$–125° (scan rate = 1°/min, step: 0.024° and Si internal standard) and found that all peaks were compatible with a rhombohedral unit cell. However, the presence of very weak reflections and/or overlaps indicative of lower symmetry cannot be ruled out without a single-crystal X-ray or electron diffraction study. Such studies are planned in the near future.

CONCLUSIONS

In summary, we have developed a facile moderate temperature route for the synthesis of good quality single crystals of rare earth perovskite manganates which should be suitable not only for resistivity and magnetic studies, but also for such physical characterizations as heat capacity, Hall measurement, resonance Raman spectroscopy, and atomic force and scanning tunneling microscopy.

The results reported in this study represent the first example of the observation of CMR effect in undoped bulk single crystals of $LaMnO_3$, $La_{0.936}Mn_{0.982}O_3$. The role of grain boundaries (GB) in the CMR effect has been investigated extensively, primarily in polycrystalline materials and in epitaxially grown manganate films (12–15, 27). There appears to be a consensus that the GB are important in the CMR effect. However, the GB contribution seems to be important only at $T \ll T_c$. The CMR is maximum at the metal–insulator transition in both polycrystalline and single-crystal materials, but appears to be much sharper and larger in single-crystal or thin film samples.

Studies of CMR of well-characterized, high-quality, relatively defect-free bulk single crystals would help to clarify GB issues and any three-dimensional aspect of the phenomenon relative to polycrystalline and thin film materials, respectively. We are currently examining the MR effects of the $LaMnO_3$ crystals doped with heterovalent ions at the La site.

ACKNOWLEDGMENTS

The work of M.G. and W.H.M. was supported in part by the National Science Foundation—Solid State Chemistry Grant DMR-96-13106. K.V.R. acknowledges the release time awarded by Rowan University under a separately budgeted research grant.

REFERENCES

1. K. Chabara, T. Ohno, M. Kasai, and Y. Kozono, *Appl. Phys. Lett*. **63,** 1990 (1993).
2. R. von Helmolt, J. Wocker, B. Holzapfel, M. Schultz, and K. Samwer, *Phys. Rev. Lett*. **71,** 2331 (1993).
3. S. Jin, T. H. Tiefel, M. McCormack, R. A. Fastnacht, R. Ramesh, and L. H. Chen, *Science* **264,** 413 (1994).
4. H. L. Ju, C. Kwon, R. L. Greene, and T. Venkatesan, *Appl. Phys. Lett*. **65,** 2108 (1994).
5. M. McCormack, S. Jin, T. H. Tiefel, R. M. Fleming, and J. M. Phillips, *Appl. Phys. Lett*. **64,** 3045 (1994).
6. C. N. R. Rao, A. K. Cheetham, and R. Mahesh, *Chem. Mater*. **8,** 2421 (1996).
7. C. Zener, *Phys. Rev*. **82,** 403 (1951).
8. M. A. Subramanian, B. H. Toby, A. P. Ramirez, W. J. Marshall, A. W. Sleight, and G. H. Kwei, *Science* **273,** 81 (1996).
9. A. P. Ramirez, R. J. Cava, and J. Krajewski, *Nature* **386,** 156 (1997).
10. A. Urishibara, Y. Moritomo, T. Arima, A. Asamitsu, G. Kido, and Y. Tokura, *Phys. Rev. B* **51**(20), 14103 (1995).
11. T. Hasimoto, N. Ishizawa, N. Mitzutani, and M. Kato, *J. Cryst. Growth* **84,** 207 (1987).
12. A. Gupta, G. O. Gong, G. Xiao, P. R. Duncombe, P. Lecoeur, P. Trouilloud, Y. Y. Wang, V. P. Dravid, and J. Z. Sun, *Phys. Rev. B* **54**(R15), 629 (1996).
13. N. D. Mathur, G. Burnell, S. P. Isaac, T. J. Jackson, B.-S. Teo, J. L. MacManus-Driscoll, L. F. Cohen, J. E. Evetts, and M. G. Blamire, *Nature* **387,** 266 (1997).
14. H. Y. Hwang, S.-W. Cheong, N. P. Ong, and B. Batlogg, *Phys. Rev. Lett*. **75,** 2041 (1996).
15. H. L. Ju and Hyunchul Sohn, *Solid State Commun*. **102,** 463 (1997).
16. W. H. McCarroll, K. V. Ramanujachary, and M. Greenblatt, *J. Solid State Chem*. **130,** 327 (1997).
17. W. H. McCarroll, K. V. Ramanujachary, J. Sunstrom, and M. Greenblatt, in press.
18. F. Licci, G. Turilli, and P. Ferro, *J. Magn. Magn. Mater*. **164,** L268 (1996).
19. J. R. Michael and R. P. Goehner, *MSA Bull*. **33,** 168 (1993).
20. B. C. Hauback, H. Fjellvag, and N. Sakai, *J. Solid State Chem*. **124,** 43 (1996).
21. A. K. Cheetham, C. N. R. Rao, and T. Vogt, *J. Solid State Chem*. **126,** 337 (1996).
22. B. C. Tofield and W. F. Scott, *J. Solid State Chem*. **10,** 183 (1974).
23. A. Gupta, T. R. McGuire, P. R. Duncombe, M. Rupp, J. Z. Sun, W. J. Gallagher, and Gang Xiao, *Appl. Phys. Lett*. **67,** 456 (1995).
24. A. Asamitsu, Y. Moritomo, Y. Tomioka, T. Arima, and Y. Tokura, *Nature* **373,** 407 (1995).
25. V. Ferris, G. Goglio, L. Brohan, O. Joubert, P. Molinie, M. Ganne, and P. Dordor, *Mater. Res. Bull*. **32,** 763 (1997).
26. A. Maignan, C. Michel, M. Hervieu, and B. Raveau, *Solid State Commun*. **101,** 277 (1997).
27. S. Jin, M. McCormack, T. H. Tiefel, and R. Ramesh, *J. Appl. Phys*. **76,** 6929 (1994).